

Document downloaded from:

<http://hdl.handle.net/10251/99363>

This paper must be cited as:

Corma Canós, A.; Moliner Marin, M.; Cantin Sanz, A.; Díaz Cabañas, MJ.; Jorda Moret, JL.; Zhang, D.; Sun, J.... (2008). Synthesis and structure of polymorph B of zeolite Beta. *Chemistry of Materials*. 20(9):3218-3223. doi:10.1021/cm8002244



The final publication is available at  
<https://doi.org/10.1021/cmS002244>

Copyright American Chemical Society

Additional Information

## Synthesis and structure of polymorph B of zeolite Beta

Avelino Corma<sup>1\*</sup>, Manuel Moliner<sup>1</sup>, Ángel Cantín<sup>1</sup>, María J. Díaz-Cabañas<sup>1</sup>, José L. Jordá<sup>1</sup>, Daliang Zhang<sup>2,4</sup>, Junliang Sun<sup>2,4</sup>, Kjell Jansson<sup>3,4</sup>, Sven Hovmöller<sup>2</sup>, Xiaodong Zou<sup>2,4\*</sup>

(1) Instituto de Tecnología Química, UPV-CSIC, Universidad Politécnica de Valencia, Avda. de los Naranjos s/n, 46022 Valencia, Spain

Tel: 34(96)3877800; Fax: 34(96)3877809; E-mail: [acorma@itq.upv.es](mailto:acorma@itq.upv.es)

(2) Structural Chemistry, Stockholm University, SE-106 91 Stockholm, Sweden

(3) Inorganic Chemistry, Stockholm University, SE-106 91 Stockholm, Sweden

(4) Berzelii Centre EXSELENT on Porous Materials, Stockholm University, SE-106 91 Stockholm, Sweden

E-mail: [zou@fos.su.se](mailto:zou@fos.su.se)

\* To whom correspondence should be addressed

**Abstract**

It has been found that it is possible to obtain either polymorph B or the C of zeolite Beta with the same structure directing agent, i.e., 4,4-dimethyl-4-azonia-tricyclo[5.2.2.0<sup>2,6</sup>]undec-8-ene hydroxide. The synthesis occurs through a consecutive process in where polymorph B is firstly formed and then transformed into polymorph C. It is possible to produce a zeolite highly enriched in polymorph B, provided that the transformation of this phase into polymorph C is slowed down up to the point that BEC is only detected at trace levels.

The structure of polymorph B has been determined by the first time by SAED and HRTEM from the areas of unfaulted polymorph B crystals.

**Keywords:** Beta Synthesis, Polymorph B, Polymorph B structure, SAED

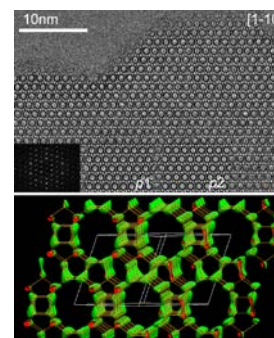
## TOC Summary and Graphic Template for Chemistry of Materials

**Avelino Corma\***, **Manuel Moliner**, **Ángel Cantín**, **María J. Díaz-Cabañas**, **José L. Jordá**, **Daliang Zhang**, **Junliang Sun**, **Kjell Jansson**, **Sven Hovmöller**, **Xiaodong Zou\***

*Chem. Mater.*

Synthesis and structure of polymorph B of zeolite Beta

By optimizing synthesis conditions, it was possible to synthesize a highly enriched polymorph B of Beta zeolite. SAED patterns from different areas and directions show that crystallites contain often twins of polymorph B and in some cases stacking faults. The twinning and stacking faults are observed more frequently near the surface than in the bulk of the crystallites. The structure of BEB has been successfully determined by SAED and HRTEM from the areas of unfaulted polymorph B crystals.



## 1.- INTRODUCTION

Zeolites are crystalline microporous materials that show interesting properties in catalysis, gas separation, and other important technological applications.<sup>[1,2]</sup> More than 200 structures<sup>[3]</sup> have been synthesized within a large spectra of pore diameters and topology networks.<sup>[4-9]</sup> The synthesis of a particular structure, when several potential structures compete, is determined by variables such as the nature of the silica source, the organic structure directing agent (OSDA), the presence of other framework elements, the gel composition and synthesis temperature. Since the crystallization of a specific material in zeolite synthesis is kinetically controlled, a thermodynamically less stable OSDA-zeolite composite can crystallize in a given system. Nevertheless, the relative stability of potentially competing nuclei towards redissolution may indicate which zeolite will preferentially be formed during the early stages of the synthesis.<sup>[10,11]</sup>

Burton has nicely shown, by molecular modeling and experimental work, the important role of the organic structure directing agent on the stabilization of a particular structure.<sup>[12]</sup> However, zeolites are metastable phases and a sequential phase transformation can occur in a series of structures of the same family that present different thermodynamic stability.

Calorimetric experiments<sup>[13]</sup> indicate that polymorph C (BEC) of Beta zeolite, either as germanate,<sup>[14]</sup> or silicogermanate<sup>[15]</sup> are more stable than Beta zeolite, which is formed by an intergrowth of polymorphs A and B (60% and 40% respectively). Nevertheless, extrapolated values for the pure silica forms indicate that Beta zeolite is more stable than polymorph C. However, one should take into account that those values were obtained for samples where the organic molecule was previously removed, and the presence of the organic molecule strongly helps to stabilize a given structure during the synthesis.<sup>[12]</sup>

Recently, a new family of materials enriched with polymorph B of the BEA family has been reported.<sup>[16,17]</sup> There, it was claimed a ratio polymorph B : polymorph A of 95:05, 75:25 and 65:35 for NCL-5, NCL-6 and NCL-7, respectively. However, no crystallographic information was given in those papers and the polymorph ratio was assigned by just comparing the XRD pattern of the samples with simulated patterns for

random intergrowths of polymorphs A and B. Nevertheless, a detailed observation of the diffractograms of NCL materials (Fig. 2 and 3 of ref. 16) shows that a considerable amount of polymorph C of Beta family is also present in all samples. That can be easily detected by the presence of a shoulder in the first peak and the two peaks observed at  $2\theta$  around  $22^\circ$  (Fig. 3 of ref. 16), one due to polymorph B and the other due to polymorph C. Taking all this into account, it appears that the results presented do not support the claims of the authors.

## 2.- EXPERIMENTAL AND DESIGN OF EXPERIMENTS

### *Synthesis of pure silica MCM-41 and Ti-MCM-41*

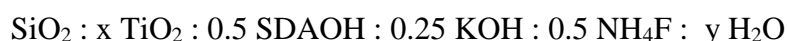
MCM-41 and Ti-MCM-41 were synthesized following the procedure described elsewhere.<sup>[18,19]</sup>

### *Synthesis of SDA*

The SDA is 4,4-dimethyl-4-azonia-tricyclo[5.2.2.0<sup>2,6</sup>]undec-8-ene hydroxide, that directs the synthesis of the pure silica ITQ-17. Its synthesis procedure is also described in previous work.<sup>[20]</sup>

### *Synthesis of ITQ-17 and Polymorph B of Beta zeolite*

The synthesis gel was prepared by mixing the silica source (Ludox AS-40 or MCM-41) with alkaline solutions of SDA(OH) and KOH. When the mixture was homogeneous, and Ludox used as silica source, titanium was added as titanium(IV) ethoxide. Finally, an aqueous NH<sub>4</sub>F solution was added, resulting in a thick gel. This was transferred to Teflon-lined stainless steel autoclaves and heated at different crystallization times. The solids were recovered by filtration, extensively washed with boiling water and dried at 100°C overnight. The general gel composition was:



### *Characterization techniques*

Powder X-ray diffraction measurements were performed with a Philips X'Pert MPD diffractometer equipped with a PW3050 goniometer, with the use of Cu-K $\alpha$  radiation and a multisample handler. Titanium and silicon were analyzed with an ICP Optical Emission Spectrometer (Varian 715-ES). Scanning electron microscopy (SEM) was

performed on a high-resolution scanning electron microscope JEOL JSM-7401F at 2.0 kV with a working distance of 2.0 mm.

#### *Structure determination*

Selected area electron diffraction (SAED) and transmission electron microscopy (TEM) were performed on a JEOL JEM-2000FX at 200 kV with a maximum tilt of  $\pm 45^\circ$  and JEM-3010 at 300 kV with a point resolution of 1.7 Å. Samples for TEM were dispersed in ethanol by ultrasound. A drop of the suspension was transferred onto a copper grid covered by holey carbon films. SAED patterns and HRTEM images were recorded on KeenView CCD cameras from Olympus Soft Imaging Solutions and a Gatan Multiscan 600HP CCD camera, respectively.

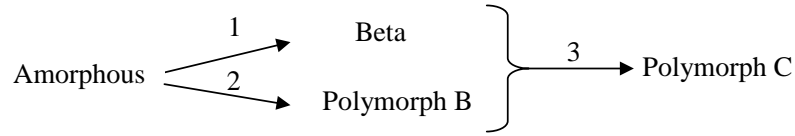
Quantification and indexation of SAED patterns were performed by the programs ELD<sup>[21]</sup> and PhIDO, respectively. Unit cell parameters were determined from a tilt series of SAED patterns by the program Trice.<sup>[22]</sup> Amplitudes and phases of the crystallographic structure factors were determined from HRTEM images by the program CRISP.<sup>[23]</sup> 3D potential maps were reconstructed using the program eMap, from which atomic coordinates of the Si atoms were determined.<sup>[24]</sup> Atomic coordinates of the Si and O atoms were refined by distance least squares refinement using the program DLS-76.<sup>[25]</sup>

### **3.- RESULTS AND DISCUSSION**

#### **3.1.- Synthesis of polymorph B of Beta family**

When we have carried out the synthesis of the pure silica polymorph C of Beta zeolite, it was observed that the formation of BEC occurs by a phase transformation from Beta more enriched with polymorph B, to the pure silica BEC structure.<sup>[20]</sup> We can then represent the global crystallization process by the consecutive transformations shown in Figure 1.

**Figure 1:** The global crystallization process can be represented by phase transformation from Beta enriched in polymorph B, to the pure silica BEC structure.



In that scheme, if one wishes to maximize the formation of the intermediate product with the highest proportion in polymorph B or, at least, to form a material highly enriched in polymorph B, process 3 should be minimized. Following this, we have here explored the variables that influence the rate of crystallization, hoping to find conditions where the transformation of B into C is preferentially slowed down. Furthermore, once favoured the formation of the intermediate product (Beta family material), it is necessary that  $2 \gg 1$  in order to produce pure polymorph B or, at least, material highly enriched in polymorph B.

**Table 1:** Synthesis conditions for the studied samples.

DIRECT SYNTHESIS <sup>a</sup>							
%wt TiO <sub>2</sub> /SiO <sub>2</sub>	H <sub>2</sub> O/Si = 7.5		H <sub>2</sub> O/Si = 15		H <sub>2</sub> O/Si = 20		14 days
	7 days	14 days	7 days	14 days	Seeding with B(85)		
					7 days	14 days	
without Ti	C-B(60)	C	B(85)	C-B(85)	B(85)	B(85)-C	Amorphous
1%wt	C-B(60)	C	B(75)-Amorp.	B(75)			
2%wt	B(60)-C	B(60)-C	Amorphous	B(65)			
4%wt	B(60)	B(60)-C	Amorphous	Amorp.-B(60)			

TRANSFORMATION OF Ti-MCM-41 <sup>a</sup>						
%wt TiO <sub>2</sub> /SiO <sub>2</sub>	H <sub>2</sub> O/Si = 7.5			H <sub>2</sub> O/Si = 15		
	7 days	14 days	30 days	7 days	14 days	30 days
without Ti	B(50)	C	C	B(55)	B(55)	B(55)-C
1%wt				B(65)-Amorp.	B(65)	B(65)-C
2%wt	B(50)	B(50)-C	C	B(85)-Amorp.	B(85)	B(85)-C
3%wt				Amorphous	Amorphous	Amorphous
4%wt				Amorphous	Amorphous	Amorphous

[a] Phase B is the intergrowth of polymorphs A:B with the ratio of B inside the brackets, determined from XRD. Phase C is the polymorph C of beta zeolite



During synthesis at a  $\text{H}_2\text{O}/\text{SiO}_2$  ratio = 7.5, an amorphous material is firstly formed that evolves into a Beta type zeolite enriched in B polymorph (60%) after 7 days (Table 1). This is transformed into polymorph C and the pure silica BEC is synthesized in 14 days. In order to decrease the rate of this transformation we increased the dilution of the gel to  $\text{H}_2\text{O}/\text{SiO}_2 = 15$ . Since all the Beta samples obtained present a higher content in polymorph B than usual Beta samples, it seems that this SDA favors the formation of polymorph B instead of A. Because of that, increasing the gel dilution should also favor the formation of the thermodynamically more stable phase, polymorph B. Indeed, at  $\text{H}_2\text{O}/\text{SiO}_2 = 15$  a material with  $85\pm 5\%$  of polymorph B and  $15\pm 5\%$  of polymorph A was produced (see Table 1 and Figure 2). This was determined by comparing the XRD pattern of the sample obtained, with simulated diffraction patterns of zeolite Beta, obtained with the DIFFaX program,<sup>[26]</sup> containing different A/B ratios (see Figure 3).

**Figure 2:** Powder X-ray diffraction pattern of most enriched Beta zeolite in polymorph B.

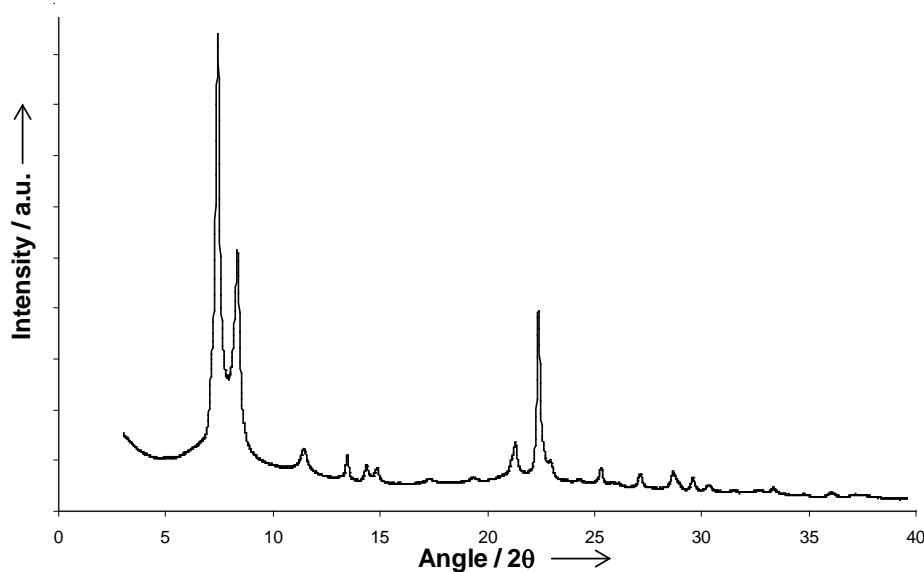
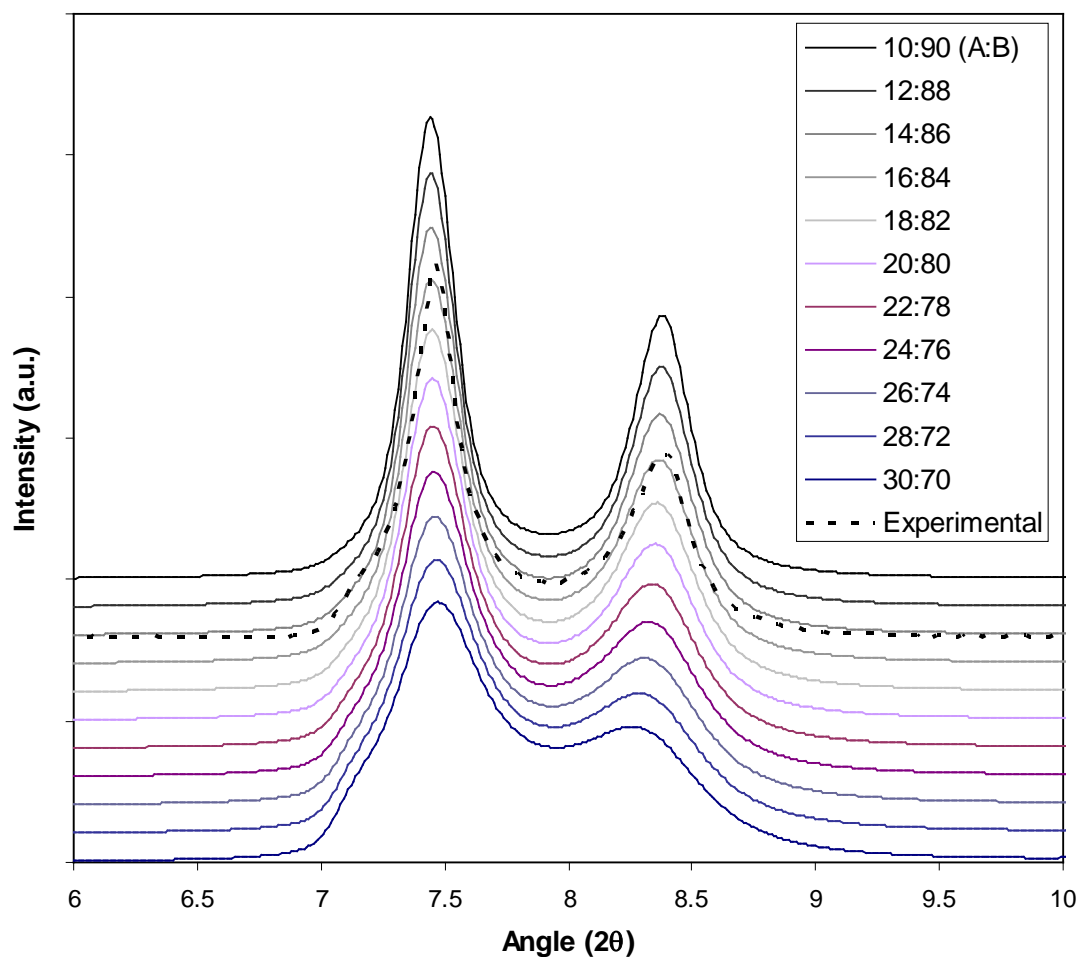
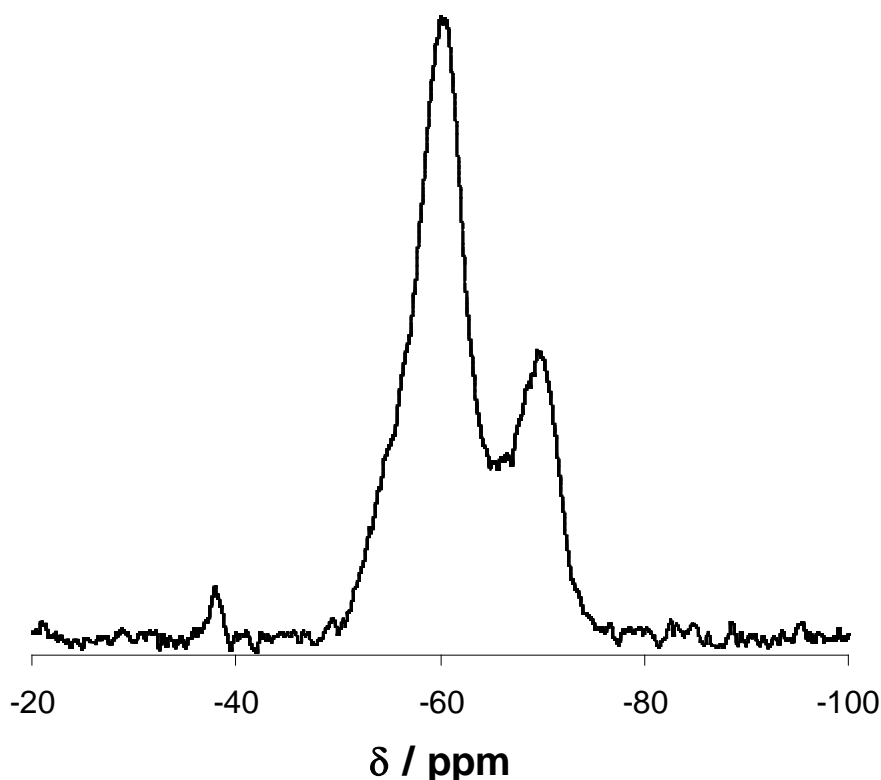


**Figure 3:** Simulation of the diffraction patterns of Beta zeolite with different ratios of polymorphs A:B, using the program DIFFaX, indicating that the material is formed by an intergrowth ratio (A:B) of 15:85.



The presence of polymorph C could not be detected by XRD in the synthesized sample described above. Nevertheless, the  $^{19}\text{F}$  MAS NMR spectrum of the as-made material of the sample enriched in polymorph B has three signals at -38.3, -60.7, and -70.3 ppm (see Figure 4). The very small signal at -38.3 ppm is assigned to the presence of fluoride anions within double 4-ring (D4R) units.<sup>[27]</sup> These secondary building units are present neither in polymorph A nor in B, but only in polymorph C. Therefore, we can say that even if polymorph C can not be detected by XRD, it is present in the polymorph B enriched material in trace amounts.

**Figure 4:**  $^{19}\text{F}$  MAS NMR spectra of the as made polymorph B enriched in Beta zeolite.



When the synthesis at  $\text{H}_2\text{O}/\text{SiO}_2 = 15$  was prolonged 14 days, some of the material enriched with polymorph B is still present, although polymorph C was the major phase observed. A further gel dilution ( $\text{H}_2\text{O}/\text{SiO}_2 = 20$ ) strongly slows down the rate of crystallization and even after 14 days only an amorphous phase was detected.

Since we have achieved a sample highly enriched in polymorph B and practically free of polymorph C, we have used that material to seed the synthesis gel ( $\text{H}_2\text{O}/\text{SiO}_2 = 15$ ) with the aim of increasing process 2, and therefore improving the formation of polymorph B. Results show that the  $85\pm 5\%$  polymorph B containing material is formed after 7 days, while at 14 days the product still contains an important amount of the  $85\pm 5\%$  polymorph B sample. It is remarkable that even when seeding, the proportion of polymorph B in the material obtained did not go beyond the  $85\pm 5\%$ .

Since the presence of Ti has been found to decrease the rate of zeolite synthesis,<sup>[28]</sup> we have introduced different levels of Ti, in the form of Ti(IV) ethoxide, within the

synthesis gel. Ti decreases the rate of crystallization of all the different polymorphs, but did not increase the content of polymorph B (see Table 1).

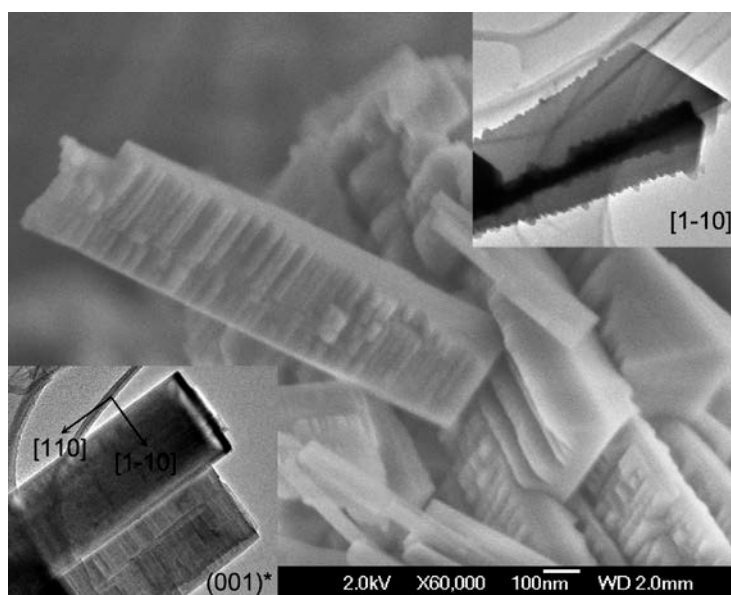
Finally, silica MCM-41 and Ti containing MCM-41 have been used as a source of silica for the synthesis (see Table 1). The rate of crystallization was decreased. Only with Ti-MCM-41 (2 wt% Ti) a sample with  $85\pm 5\%$  of polymorph B was obtained.

A pure silica sample with 85% content in polymorph B has been used to determine the crystalline structure of polymorph B.

### 3.2.- Determination of polymorph B structure

The polymorph B enriched sample was studied by both scanning electron microscopy (SEM) and transmission electron microscopy (TEM). The crystals were rod-like with the longest dimension ( $0.5\mu\text{m}\sim 2\mu\text{m}$ ) along [110] and the other two dimensions along [1-10] and  $c^*$  axis ( $0.1\mu\text{m}\sim 0.4\mu\text{m}$ ) (see Figure 5). As noted already by Newsam et al.,<sup>[29]</sup> the crystal surfaces are not smooth. A large number of sharp ridges are formed perpendicular to the long [1-10] direction, as is evident in the SEM image (Figure 5). The crystals are slightly wedge-shaped.

**Figure 5:** SEM image showing the morphology of polymorph B crystals. Inserts are TEM images showing that the crystals are wedge-shaped in the [1-10] projection (top-right) and rectangular in the  $c^*$  projection (bottom-left).

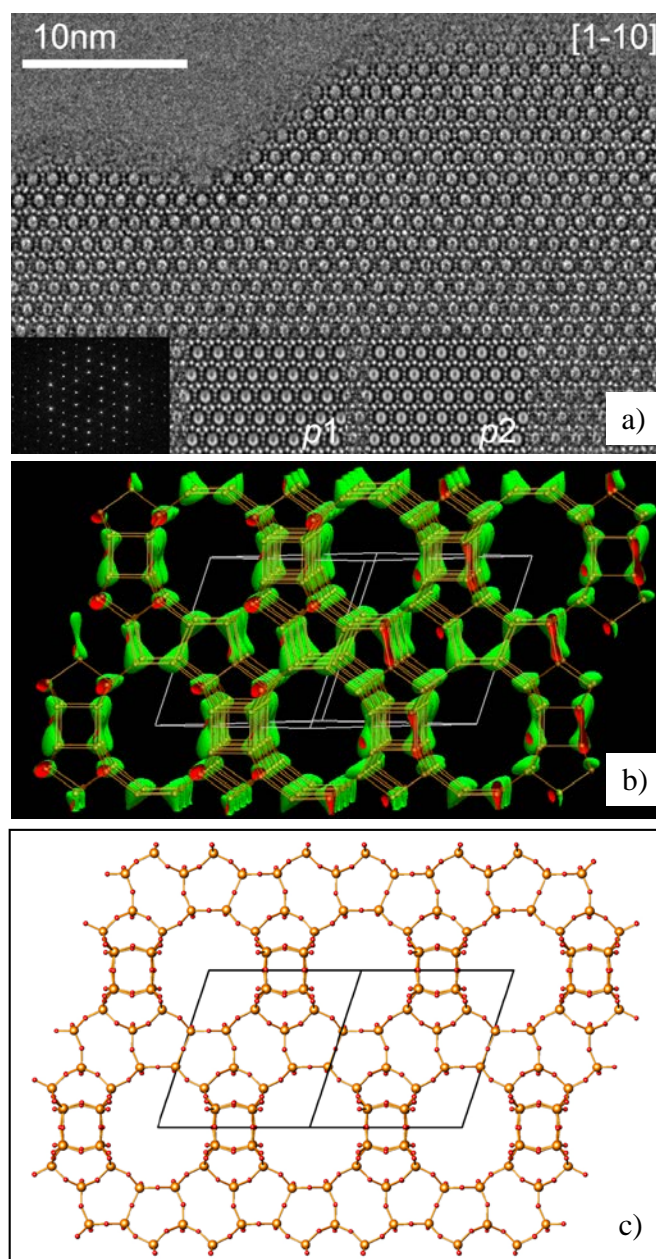


Selected area electron diffraction (SAED) patterns from different areas and different directions show that most crystallites contain twins of polymorph B indicated by twinned SAED patterns or stacking faults indicated by streaks in the SAED patterns. In general, the twinning and stacking faults were observed more frequently near the surface than in the bulk of the crystallites. The unfaulted polymorph B crystals are large enough for a complete structure determination of polymorph B by SAED and high resolution transmission electron microscopy (HRTEM). The structure solution is presented below.

The unit cell of polymorph B was determined from a tilt series of SAED patterns, using the programs ELD<sup>[21]</sup> and Trice.<sup>[22]</sup> The unit cell parameters were  $a = 17.97 \text{ \AA}$ ,  $b = 17.97 \text{ \AA}$ ,  $c = 14.82 \text{ \AA}$ ,  $\alpha = 90^\circ$ ,  $\beta = 113.7^\circ$  and  $\gamma = 90^\circ$ . The possible space groups were  $Cc$  and  $C2/c$ , deduced from the reflection conditions observed from the SAED patterns:  $hkl: h + k = 2n$ ;  $h0l: h = 2n, l = 2n$ ;  $0k0: k = 2n$ .

HRTEM images of polymorph B taken along the [1-10] direction show clearly 12-ring channels arranged in ABCABC... stacking sequence, characteristic of the polymorph B structure (Figure 6a). The lattice averaged projection derived from the HRTEM images shows 2-fold symmetry, and is consistent with the space group  $C2/c$  (Figure 6a). Well resolved 4-, 5-, and 6- rings are observed from the HRTEM images.

**Figure 6:** (a) HRTEM image along the  $[1-10]$  direction used for structure determination. Except for one row on the top left of the crystal, the crystal along the projection is perfect. Only the area without any defects was used for structure determination. Inserts are (from left to right) Fourier transform of this area and average images with  $p1$  and  $p2$  symmetries. (b) The 3D potential map reconstructed from this HRTEM image. All 9 unique Si atoms were found and their atomic coordinates were determined from this 3D map. (c) Structure model of polymorph B after distance-least square refinement. Si atoms are in yellow and O atoms in red.



Structure determination was made from the thinnest area of the polymorph B crystal in the HRTEM image (Figure 6a). Because of the symmetry, HRTEM images taken along the [1-10] direction are equivalent to those taken along the [110] direction. These directions are 90° from each other. Thus it is possible to obtain a complete 3D structure of polymorph B from the single [1-10] projection. Amplitudes and phases of the crystallographic structure factors of 39 independent reflections with  $d > 2.5 \text{ \AA}$  were extracted from the [1-10] HRTEM images by the program CRISP.<sup>[23]</sup> These 39 reflections further generated a total of 152 reflections that were used for reconstructing the 3D potential map (Figure 6b). All nine Si atoms could be resolved from the 3D potential map made by the program eMap (Table 2).<sup>[24]</sup> Each of them was connected to four other Si atoms, resulting in a 3D framework (Figure 6b).

**Table 2:** Atomic coordinates of Si obtained from the 3D potential map reconstructed from the HRTEM images.

Atoms	$x_{EM}^*$	$y_{EM}^*$	$z_{EM}^*$	Dev( $\text{\AA}$ ) <sup>**</sup>
Si1	0.62	0.97	0.41	0.41
Si2	0.49	0.84	0.41	0.46
Si3	0.69	0.69	0.60	0.42
Si4	0.83	0.84	0.61	0.11
Si5	0.57	0.82	0.61	0.31
Si6	0.71	0.95	0.61	0.15
Si7	0.50	0.88	0.75	0.17
Si8	0.69	0.90	0.24	0.32
Si9	0.50	0.70	0.25	0.43

\* The standard deviations for the coordinates are estimated to be 0.01.

\*\* The deviations were calculated by comparing atomic positions with those refined by DLS-76.

Oxygen atoms could not be resolved at this resolution of the HRTEM images but were inserted geometrically between the neighboring Si atoms. The nine Si and sixteen O positions were then refined by distance least squares refinement using the program DLS-76.<sup>[25]</sup> The unit cell parameters were also refined by DLS-76 to be  $a = 17.70 (15) \text{ \AA}$ ,  $b = 17.70 (15) \text{ \AA}$ ,  $c = 14.33 (11) \text{ \AA}$ , and  $\beta = 114.89 (1)^\circ$ . The final structure model of polymorph B (Figure 6c, and Table 3) agrees with those proposed in the literature.<sup>[3,29,30]</sup>

*Table 3: Atomic coordinates of polymorph B refined by DLS-76.*

Atoms	$x$	$Y$	$z$
Si1	0.606(3)	0.979(3)	0.381(4)
Si2	0.482(2)	0.857(3)	0.377(3)
Si3	0.699(3)	0.711(2)	0.606(4)
Si4	0.826(2)	0.834(2)	0.613(3)
Si5	0.580(3)	0.834(3)	0.610(4)
Si6	0.704(3)	0.957(2)	0.615(4)
Si7	0.5	0.889(4)	0.75
Si8	0.695(3)	0.916(2)	0.254(5)
Si9	0.5	0.724(4)	0.25
O1	0.533(4)	0.919(4)	0.348(5)
O2	0.650(4)	0.988(4)	0.503(4)
O3	0.571(3)	1.060(3)	0.332(4)
O4	0.674(4)	0.954(4)	0.341(6)
O5	0.512(4)	0.854(4)	0.499(4)
O6	0.385(3)	0.875(5)	0.327(7)
O7	0.496(6)	0.775(4)	0.339(3)
O8	0.773(4)	0.768(3)	0.629(5)
O9	0.622(4)	0.753(3)	0.612(7)
O10	0.732(4)	0.646(3)	0.692(6)
O11	0.670(4)	0.673(3)	0.496(5)
O12	0.786(3)	0.915(3)	0.620(5)
O13	0.919(2)	0.829(4)	0.702(5)
O14	0.652(4)	0.896(3)	0.646(5)
O15	0.539(4)	0.836(3)	0.691(5)
O16	0.728(4)	1.024(3)	0.697(6)

The polymorph B structure is built from a building layer consisting of 12-rings. Adjacent layers are related by an inversion centre (i) located between the layers. The 12-ring pores are shifted from each other and packed in an ABCABC... stacking



sequence. The structure of polymorph B contains intersecting channels in 3 directions, with straight 12-ring channels along [110] and [1-10], and inclined 12-ring channels along [001].

#### **4.- Conclusions**

In conclusion, we have found that the very same organic SDA that directs towards formation of the BEC polymorph can selectively form, in a preceding synthesis step samples of Beta zeolite enriched in polymorph B. By optimizing the synthesis conditions it was possible to produce a zeolite highly enriched in polymorph B, provided that the transformation of this phase into polymorph C is slowed down, up to the point that BEC is only detected at trace level. SAED patterns from different areas and directions show that most crystallites contain twins of polymorph B or stacking faults. The twinning and stacking faults are observed more frequently near the surface than in the bulk of the crystallites. The structure of polymorph B has been successfully determined by SAED and HRTEM from the areas of unfaulted polymorph B crystals.

## **Acknowledgements**

Financial support from Spanish government (Project MAT2006-14274-C02-01) and EU Commission (TOPCOMBI Project) are gratefully acknowledged, MM thanks to CSIC for an I3P grant. J.-L. Sun is supported by a post doctoral grant from the Carl-Trygger Foundation. The Berzelii Centre EXSELENT is financially supported by the Swedish Research Council (VR) and the Swedish Governmental Agency for Innovation Systems (VINNOVA).

## Figure Captions

**Figure 1:** The global crystallization process can be represented by phase transformation from Beta enriched in polymorph B, to the pure silica BEC structure.

**Figure 2:** Powder X-ray diffraction pattern of most enriched Beta zeolite in polymorph B.

**Figure 3:** Simulation of the diffraction patterns of Beta zeolite with different ratios of polymorphs A:B, using the program DIFFaX, indicating that the material is formed by an intergrowth ratio (A:B) of 15:85.

**Figure 4:**  $^{19}\text{F}$  MAS NMR spectra of the as made polymorph B enriched in Beta zeolite.

**Figure 5:** SEM image showing the morphology of polymorph B crystals. Inserts are TEM images showing that the crystals are wedge-shaped in the [1-10] projection (top-right) and rectangular in the  $c^*$  projection (bottom-left).

**Figure 6:** (a) HRTEM image along the [1-10] direction used for structure determination. Except for one row on the top left of the crystal, the crystal along the projection is perfect. Only the area without any defects was used for structure determination. Inserts are (from left to right) Fourier transform of this area and average images with  $p1$  and  $p2$  symmetries. (b) The 3D potential map reconstructed from this HRTEM image. All 9 unique Si atoms were found and their atomic coordinates were determined from this 3D map. (c) Structure model of polymorph B after distance-least square refinement. Si atoms are in yellow and O atoms in red.

## Table Captions

**Table 1:** Synthesis conditions for the studied samples.

**Table 2:** Atomic coordinates of Si obtained from the 3D potential map reconstructed from the HRTEM images.

**Table 3:** Atomic coordinates of polymorph B refined by DLS-76.

## References

- [1] Davis, M. E. *Nature*. **2002**, *417*, 813-821.
- [2] Corma, A. *J. Catal.* **2003**, *216*, 298-312.
- [3] IZA structure commission, [www.iza-structure.org](http://www.iza-structure.org).
- [4] Strohmaier, K. G.; Vaughan, D. E. *J. Am. Chem. Soc.* **2003**, *125*, 16035-16039.
- [5] Burton, A.; Elomari, S.; Chen, C-Y.; Medrud, R. C.; Chan, I. Y.; Bull, L. M.; Kibby, C.; Harris, T. V.; Zones, S. I.; Vittoratos, E. S. *Chem. Eur. J.* **2003**, *9*, 5737-5748.
- [6] a) Paillaud, J. L.; Harbuzaru, B.; Patarin, J.; Bats, N. *Science*. **2004**, *304*, 990-992. b) Corma, A.; Diaz-Cabañas, M. J.; Rey, F.; Nicolopoulos, S.; Boulahya, K. *Chem. Commun.* **2004**, 1356-1357.
- [7] Corma, A.; Rey, F.; Rius, J.; Sabater, M. J.; Valencia, S. *Nature*. **2004**, *431*, 287-290.
- [8] Corma, A.; Diaz-Cabañas, M. J.; Martinez-Triguero, J.; Rey, F.; Rius, J. *Nature*. **2002**, *418*, 514-517.
- [9] Corma, A.; Diaz-Cabañas, M. J.; Jordá, J. L.; Martinez, C.; Moliner, M. *Nature*. **2006**, *443*, 842-845.
- [10] Sastre, G.; Leiva, S.; Sabater, M. J.; Gimenez, I.; Rey, F.; Valencia, S.; Corma, A. *J. Phys. Chem. B.* **2003**, *107*, 5432-5440.
- [11] Lowe, B. M. *Zeolites*. **1983**, *3*, 300-305.
- [12] Burton, A. W. *J. Am. Chem. Soc.* **2007**, *129*, 7627-7637.
- [13] Li, O.; Navrotsky, A.; Rey, F.; Corma, A. *Microp. Mesopor. Mater.* **2003**, *59*, 177-183.
- [14] Conradson, T.; Dadachov, M. S.; Zou, X. D. *Microp. Mesopor. Mater.* **2000**, *41*, 183-191.

- [15] Corma, A.; Navarro, M. T.; Rey, F.; Rius, J.; Valencia, S. *Angew. Chem. Int. Ed.* **2001**, *40*, 2277-2280.
- [16] Kadgaonkar, M. D.; Kasture, M. W.; Bhange, D. S.; Joshi, P. N.; Ramasway, V.; Kumar, R. *Microp. Mesopor. Mater.* **2007**, *101*, 108-114.
- [17] Kadgaonkar, M. D.; Kasture, M. W.; Bhange, D. S.; Joshi, P. N.; Ramasway, V.; Gupta, N. M.; Kumar, R. *Microp. Mesopor. Mater.* **2007**, *105*, 82-88.
- [18] Corma, A.; Domine, M.; Gaona, J. A.; Jorda, J. L.; Navarro, M. T.; Rey, F.; Perez-Pariente, J.; Tsuji, J.; McCulloch, B.; Nemeth, L. T. *Chem. Commun.* **1998**, *20*, 2211-2212.
- [19] Blasco, T.; Corma, A.; Navarro, M. T.; Perez-Pariente, J. *J. Catal.* **1995**, *156*, 65-74.
- [20] Cantin, A.; Corma, A.; Díaz-Cabañas, M. J.; Jorda, J. L.; Moliner, M.; Rey, F. *Angew. Chem. Int. Ed.* **2006**, *45*, 8013-8015.
- [21] Zou, X. D.; Sukharev, Y.; Hovmöller, S. *Ultramicroscopy.* **1993**, *49*, 147-158.
- [22] Zou, X. D.; Hovmöller, A.; Hovmöller, S. *Ultramicroscopy.* **2004**, *98*, 187-193.
- [23] Hovmöller, S. *Ultramicroscopy.* **1992**, *41*, 121-135.
- [24] Oleynikov, P. <http://www.analitex.com>.
- [25] Baerlocher, Ch.; Hepp, A.; Meier, W. M. *DLS-76: Distance-least-squares refinement program*, ETH Zurich, Switzerland, **1976**.
- [26] Treacy, M. M. J.; Deem, M. W.; Newsam, J. M. *DIFFaX: A computer program for calculating diffraction from faulted crystals.* **1997**.
- [27] Caultlet, P.; Guth, J. L.; Hazm, J.; Lamblin, J. M.; Gies, H. *Eur. J. Solid State Inorg. Chem.* **1991**, *28*, 345-361.
- [28] Reddy, J. S.; Kumar, R. *Zeolites.* **1992**, *12*, 95-100.

[29] Newsam, J. M.; Treacy, M. M. J.; Koetsier, W. T.; de Gruyter, C. B. *Proc. R. Soc. Lond. A*. **1988**, *420*, 375-405.

[30] Treacy, M. M. J.; Newsam, J. M. *Nature*. **1988**, *332*, 249-251.